AD-A035 676

MATERIALS FOR VOLUME PHASE HOLOGRAPHY

RCA LABORATORIES, PRINCETON, NEW JERSEY

DECEMBER 1976

REPORT DOCUMENTATION PAGE		READ INSTRUCTIONS BEFORE COMPLETING FORM
1. REPORT NUMBER	2. GOVT ACCESSION NO.	3. RECIPIENT'S CATALOG NUMBER
4. TITLE (and Subtitle) MATERIALS FOR VOLUME PHASE HOLOGRAPHY		5. TYPE OF REPORT & PERIOD COVERED Final Report (10-8-75 to 10-7-76)
		6. PERFORMING ORG. REPORT NUMBER PRRL-76-CR-57
7. AUTHOR(s) William Phillips, William J. Burke, and David L. Staebler		8. CONTRACT OR GRANT NUMBER(s) N00019-76-C-0116
9. PERFORMING ORGANIZATION NAME AND ADDRESS RCA Laboratories Princeton, New Jersey 08540		10. PROGRAM ELEMENT, PROJECT, TASK AREA & WORK UNIT NUMBERS
11. CONTROLLING OFFICE NAME AND ADDRESS Naval Air Systems Command Department of the Navy Washington, DC		12. REPORT DATE December 1976
		13. NUMBER OF PAGES 56
14. MONITORING AGENCY NAME & ADDRESS (If different from Controlling Office)		15. SECURITY CLASS. (of this report) Unclassified
		15a. DECLASSIFICATION/DOWNGRADING SCHEDULE N/A

16. DISTRIBUTION STATEMENT (of this Report)

**APPROVED FOR PUBLIC RELEASE:
DISTRIBUTION UNLIMITED**

17. DISTRIBUTION STATEMENT (of the abstract entered in Block 20, if different from Report)

18. SUPPLEMENTARY NOTES

19. KEY WORDS (Continue on reverse side if necessary and identify by block number)

Phase holograms

$LiNbO_3$:Fe

20. ABSTRACT (Continue on reverse side if necessary and identify by block number)

This report describes work on single-crystal $LiNbO_3$:Fe for volume holographic information storage. The purpose was to determine if increased rates of fixing of holograms could be obtained by codoping the crystals with Si. Our conclusion is that the addition of Si to the crystal may indeed increase the fixing rate. However, large amounts of Si are required to produce the effect, and under these conditions

DD $_{1\ JAN\ 73}^{FORM}$ **1473**

20.

it appears that it will be extremely difficult to obtain higher crystal quality.

We believe that the material of choice for high density read-only information storage is $LiNbO_3$ single-doped with Fe. Up to 1000 high resolution holograms can be stored in a $6-cm^3$ crystal.

PREFACE

This final report describes research performed under contract
No. N00019-76-C-0116 at RCA Laboratories, Princeton, New Jersey. This
work was performed from 8 October 1975 to 7 October 1976 in the Commu-
nications Research Laboratory, K. Powers, Director. The Project Super-
visor is B. Williams, and the Principal Investigator is W. Phillips.
W. J. Burke and D. L. Staebler participated in the research and writing
of this report.

DDC
RECEIVED
FEB 15 1977
D

TABLE OF CONTENTS

TABLE OF CONTENTS (Continued)

LIST OF ILLUSTRATIONS

PART 1: FIXING ION RESEARCH

I. INTRODUCTION

During the past 5 years we have conducted a series of investigations
that led to the discovery and subsequent improvement of $LiNbO_3$:Fe as a phase
holographic storage medium. Phase holograms are recorded in this material
by photo-excitation of electrons trapped at Fe^{2+} sites [1] with subsequent
drift or diffusion of the electrons from regions of high light intensity
in the interference pattern of the light beams into regions of lower light
intensity. This space-charge pattern modulates the index of refraction
through the electro-optic effect, producing the phase grating. The usefulness
of holograms recorded in this way was greatly extended by the development of
a simple procedure [2] by which the holograms could be replicated as permanent
ionic patterns. This fixing procedure makes use of the fact that heating the
crystal in which the hologram is stored to between 100° and 200°C allows trans-
port of an ionic species to neutralize the electronic space-charge pattern.
Upon cooling to room temperature and redistributing the electronic space-charge
pattern with incoherent light, a hologram due to the ionic space-charge pattern
remains and can be read out until the crystal is again heated past 200°C. This
technique is the only practical existing one for the fixing of phase holograms
in a truly thick, high capacity inorganic storage medium.

A key element in the storage of fixed holograms in $LiNbO_3$ is the presence
of an ionic species which is mobile in the 100° to 200°C temperature range.
The transport behavior of these ions is extremely important since thermal
and optical erasure of previously recorded and fixed holograms takes place
while a new one is being stored. The relative rates of hologram fixing
and erasure determine the number and diffraction efficiency of the final
fixed holograms, i.e., they determine the storage capacity.

1. D. L. Staebler, W. Phillips, and B. W. Faughnan, *Materials for Phase
    Holographic Storage*, Final Report, Contract No. N00019-72-C-0147,
    prepared for Naval Air Systems Command, March 1973.
2. D. L. Staebler and J. J. Amodei, Ferroelectrics 3, 107 (1972);
    J. J. Amodei and D. L. Staebler, Appl. Phys. Letter 18, 540 (1971).

Many benefits would follow from the identification of the fixing ions, particularly if it is possible to increase the rate at which fixing takes place at any given temperature. This could be exploited to allow more holograms to be fixed in a crystal or to produce higher diffraction efficiency holograms, thus reducing the readout laser size and the buildup of spurious optical damage.

Until recently, very little was known about the exact nature of the mobile ionic species. In 1974, an experiment, described in detail in Refs. 3 and 4, was devised to attempt to identify this species. Briefly, a region of a $LiNbO_3$:Fe crystal near a c-face of the crystal was illuminated with intense laser radiation while it was hot enough for ionic motion to take place. Due to the built-in electric field in $LiNbO_3$, an excess of the fixing ion would be accumulated at the surface of the crystal where it could be identified using electron microprobe analysis. With this procedure it was discovered that Si was transported to the surface of crystals heavily doped with Fe. No other ions were found that could be implicated in the fixing process.

This result did not automatically mean that Si was responsible for the fixing. First, the electron probe microanalysis technique used to identify the Si is insensitive to ions with atomic numbers less than 12. Secondly, concentrations of intrinsic lattice defects, such as interstitial Li or oxygen vacancies, could not be detected in the quantities expected to accumulate on the surface if they were involved in the fixing [3,4]. Nevertheless, because of the strong indication that Si might be involved in the fixing process and because of the potential for improvement of the properties of the $LiNbO_3$:Fe, we embarked upon an investigation (1) to confirm or refute the possibility that Si was involved in the fixing process, and (2) to identify any other ions that might be involved in the fixing process.

In Part 1 of this report we describe the research of the past year aimed at the above objectives. In Part 2, we summarize the properties of the $LiNbO_3$:Fe materials developed over the last 5 years that are relevant to

3. B. F. Williams, W. J. Burke, and D. L. Staebler, Appl. Phys. Letters 28, 224 (1976).
4. W. Burke, W. Phillips, D. L. Staebler, and B. F. Williams, *Materials for Phase Holographic Storage*, Final Report, Contract No. N00019-74-C-0312, prepared for Naval Air Systems Command, April 1975.

information storage and retrieval, and we discuss considerations pertinent to the application of volume holographic storage to the Navy's moving map display system.

II. EXPERIMENTAL CONSIDERATIONS AND SAMPLE PREPARATION

A. APPROACH

The direct identification of the mobile ionic species responsible for
fixing in $LiNbO_3$:Fe is frustrated by the low concentrations which are
involved in the process. Only $\sim 10^{16}$ ions/cm^3 need be present to screen the
electronic charge pattern of a hologram. Many trace impurities as well as
intrinsic lattice defects are available in these concentrations in the
cyrstals. The experiment which identified Si as a mobile ion in $LiNbO_3$ was
an attempt to make a direct observation of the fixing ion by sweeping it to
the surface in large concentrations. The research of the past year was
undertaken in order to clarify the role played by Si, and to investigate
other possible fixing ion candidates by measuring their effect on the trans-
port properties of the crystals.

To accomplish this, we prepared crystals of $LiNbO_3$:Fe in which we
attempted to incorporate increased concentrations of several likely fixing
ion candidates. We then measured the fixing rate and the ionic conductivity
of these samples. This procedure would identify the ion responsible for the
fixing process if two conditions are met. The first is that the ionic con-
ductivity (and thus the fixing rate) is indeed limited by the concentration
of this ion in the crystal, so that increasing its concentration causes the
fixing rate to increase. This is a useful working assumption to make because
the goal of the program is to produce crystals which enhanced fixing times,
and such ions would be identified immediately by the above procedure. The
second condition is that we are successful in increasing the concentration of
the candidate ion. This can be verified for some, but not for all, of the
candidates we studied.

B. CHOICE OF POSSIBLE FIXING IONS

In addition to Si, which is suggested by direct experimental observation,
a number of other possibilities exist for the dominant mobile ion in the
160°C temperature range. The most likely intrinsic lattice defects are
oxygen vacancies and interstitial Li. These species are known to be highly

4

mobile at elevated temperatures both from the research of others [5] and from the following observation: when Fe-doped $LiNbO_3$ is annealed in an oxygen-deficient atmosphere at temperatures as low as $600°C$, the concentration of Fe^{2+} is increased as indicated by increased optical absorption. The mechanism for this is understood to be the evaporation of oxygen from the surface of the crystal, leaving behind two electrons for each oxygen atom. These electrons are trapped by the Fe^{3+} ions, converting them to Fe^{2+}. The mechanism for diffusion of oxygen to the surface of the crystal involves movement of oxygen vacancies. The activation energy for this process is given by Jorgensen and Bartlett [5] as 1.3 eV, which is also roughly the activation energy for hologram fixing.

Li ions are also highly mobile at elevated temperatures. This is known from the fact that Li diffuses into $LiNbO_3$ in the 400° to 600°C range and causes Fe^{3+} to become reduced to Fe^{2+}. Rough calculations give an activation energy for this process in the 1- to 1.5-eV range. We believe that, for the Li diffusion process, interstitial Li^+ is the diffusant.

Still another possibility to be considered is that an impurity ion other than Si is involved. Likely candidates would have atomic numbers less than 12, and thus would have been missed by the microprobe experiment that identified Si. In particular, Mg^{++} would be expected to have diffusion properties quite similar to Li^+ due to the similarity of its ionic radius (0.65 Å) to that of Li (0.60 Å). Mg has been found in all $LiNbO_3$ crystals in the 1- to 10-ppm range.

The above species, Li, oxygen vacancies, Si, and Mg have been incorporated in $LiNbO_3$:Fe crystals and investigated during the course of this program. The results of these examples will be discussed in subsequent subsections.

C. PREPARATION OF SAMPLES

Most of the crystals used in this program were grown at RCA Laboratories by the Czochralski method, using apparatus that has been described in an

5. P. J. Jorgensen and R. W. Bartlett, J. Phys. Chem. Solids 30, 2639 (1969).

earlier report [6]. The others were purchased from Crystal Technology, Inc. The melts from which the RCA crystals were grown consisted of about 2 moles of $LiNbO_3$ held in 100-ml platinum crucibles, plus the desired dopants in the form of oxides (e.g., MgO, SiO_2, etc.). The crystals were grown in the c-direction at rates from 0.10 to 0.20 in. per hour. Upon completion of growth they were poled by annealing in an electric field, cut to the desired size, and individual pieces were heat-treated to produce an optical density of about 0.3 at 4880 Å.

1. Preparation of Si-Doped Crystals

The ease with which Li and transition elements can be incorporated into $LiNbO_3$ by diffusion led us to attempt first to incorporate Si into $LiNbO_3$:Fe by diffusion methods. An increase in the Si concentration was obtained by coating crystals with 1000 Å of elemental Si, allowing diffusion to occur by annealing in vacuum at temperatures near 1000°C for 48 h, and then re-oxidizing the crystals. Crystals prepared this way developed a yellow color, which could not be removed by subsequent annealing. This suggests that Si incorporated by this method also stablizes a color center and tends to confirm that Si actually diffused into the crystals. The Si concentration of the diffused crystals was found to be ∿15 ppm. The absorption spectrum of a diffusion-doped crystal is shown in Fig. 1. The absorption due to Fe^{2+} in a normal $LiNbO_3$:Fe crystal is shown for comparison purposes.

To gain greater control over the Si concentration, we grew the remainder of the Si-doped crystals from the melt. The procedure we followed was to first grow a Fe-doped crystal from a melt with no Si added, then to restore the melt to its original composition and weight, add Si, and grow another crystal differing from the first only by the presence of Si. In some cases the material used in the growth of the Si-doped crystal was replaced and an additional crystal grown before the melt was discarded. In particular, sample 03239 was grown from the same melt as 03231. The additional Si in this case was added as Li_2SiO_3 instead of SiO_2.

6. J. J. Amodei, W. Phillips, and D. L. Staebler, *Phase Holographic Storage Media for Display Applications*, Final Report, Contract No. N62269-70-C-0372, June 1971.
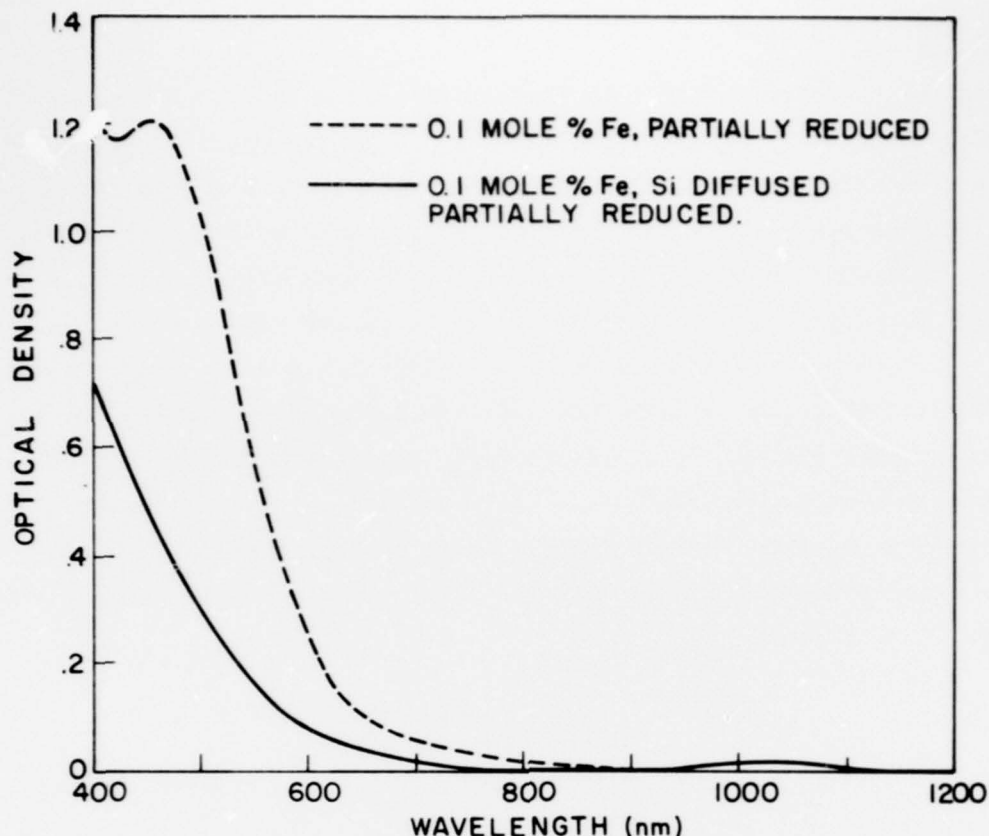
Figure 1.   Absorption spectra of a 0.1 mole % Fe-doped
crystal and a similar crystal after Si diffu-
sion and slight reduction.

Crystal chemistry arguments suggest that the solubility of Si in $LiNbO_3$ will be extremely low. The small ionic radius of Si^{4+} (0.41 Å) is a poor match for Nb^{5+} (0.70 Å) where it might otherwise situate substitutionally on the basis of charge. Both the size and the charge difference between Si^{4+} and Li^+ (0.60 Å) preclude its occupying this site in significant quantities.

Extreme difficulty was indeed encountered growing Si-doped crystals with all but the smallest amount of Si added to the melt. The crystals tended to contain large numbers of voids (gas inclusions) arrayed in the growth direction. This is indicative of large amounts of material being rejected at the growth interface.

2. Analysis of Samples for Si

Samples prepared during this project have been routinely analyzed for Si by semi-quantitative emission spectroscopy. This technique gives an indication that in virtually all samples Si is present in the 1- to 10-ppm range. Since this method of analysis is only "semi-quantitative," we tried to use other analytic techniques as well. Spark source and secondary ion mass spectroscopy were both attempted, but were unusable due to interferences in the mass spectrum (arising from a particular Li_2O isotope). Emission spectroscopy was therefore repeated utilizing standards formulated from pure $LiNbO_3$ and SiO_2 to calibrate the photographic plates. The results for the Si-doped crystals prepared during this program are shown in Table 1. The results for the more heavily doped crystals were found to be reproducible among several different samples. Conversion factors relating parts per million by weight to mole percent are given in Table 2.

TABLE 1. Fe AND Fe-Si DOPED CRYSTALS
MELT DOPING (MOLE %)

Crystal No.	Melt Doping (Mole %)		Measured Doping Level (ppm by Weight)	
	Fe	Si	Fe	Si
03227	0.01	0.003	(50)*	25 ± 8
03229	0.02	0.003	(100)*	15 ± 8
03231	0.05	0.033	270 ± 20	7 ± 2
03239	0.05	0.1	50 − 20	0.3 − 3
03244	0.05	1.0	220 ± 80	250 ± 65
03249	0.05	0	250 ± 70	15 ± 10
03250	0.05	0.5	240 ± 80	50 ± 20
03256	0.05	1.0	383 ± 35	75 ± 37

___
*Estimated.

TABLE 2. CONVERSION FACTORS FOR $LiNbO_3$

1 ppm by weight of Fe = 2.65×10^{-4} mole % Fe

1 ppm by weight of Si = 5.26×10^{-4} mole % Si

Several comments are in order about the data in Table 1. First, note that the background level of the Si determinations is in the neighborhood of 10 ppm. We cannot be sure if this amount of Si is present in all crystals or if it is an artifact of the measurement technique. The low solubility of Si in $LiNbO_3$ makes the latter seem more likely (see below).

A second point is that Si has very low solubility in the crystals. Only the three most heavily doped crystals had Si concentrations significantly above the 10-ppm background level. A crystal was grown with Si added to the melt as Li_2SiO_3 instead of SiO_2 to determine if this would increase the amount of Si in the crystals; it did not.

There is a discrepancy in the doping results for the more heavily doped crystals. Two of these crystals, 03250 and 03256, were grown successively from the same $LiNbO_3$ batch and doped with 0.5 mole % Si and with 1 mole % Si, respectively. The assigned Si concentrations are consistent with each other and correspond to about 4% of the Si concentration in the melt.

The other heavily doped crystal, 03244, was grown from a different $LiNbO_3$ melt and doped with 1 mole % Si; it contains a factor of four more Si than 03256. The silicon determinations for these crystals were reproduced in several different measurements and appear to be quite reliable. Thus the difference is in the solid solubility of Si in the two cases. This discrepancy is important because of the fixing rate results for these crystals to be discussed in Section III.

D. PREPARATION OF CRYSTALS WITH ENHANCED CONCENTRATIONS OF LATTICE DEFECTS

The incorporation of Li^+ in the crystals was attempted by packing un-polished $LiNbO_3$:Fe crystals in powdered Li_2CO_3 and annealing for two days at about 575°C. In this procedure, the mechanism involved is the diffusion of Li into the crystal. The technique has been in common use to convert Fe^{3+} to Fe^{2+} in $LiNbO_3$ crystals and to improve the optical properties of $LiNbO_3$-$LiTaO_3$ optical waveguides [7]. The concentration of Li incorporated is on the order of 0.25 mole % since this procedure reduces all of the Fe to the divalent state in crystals containing up to this overall concentration of Fe.

7. W. Phillips and J. M. Hammer, J. Electronic Materials 4, 549 (1975).

Changes in the oxygen vacancy concentration occur when the crystals are annealed in oxygen-rich or oxygen-poor atmospheres. Such anneals are used to adjust the Fe^{2+} concentration of the crystals to produce an optical density of about 0.3 for overall Fe concentration between 0.01 and 0.25%. However, significant differences in the fixing times do not occur for these crystals. Thus, if oxygen vacancies are involved in ionic fixing at all, we have to make much larger variations in their concentration to see any effect.

An estimate of the concentration of oxygen vacancies that might be needed to produce a measurable effect can be obtained from consideration of the composition of congruent $LiNbO_3$ crystals. Congruent $LiNbO_3$ is nearly 6 mole % deficient in Li; thus it can be described approximately by the formula $Li_{0.94}NbO_{2.97}$. Little is known about the details of the disorder of crystals having the congruent composition. It is thought that some of the extra Nb ions occupy Li sites, producing a nearly filled crystal structure. For the present purpose, however, we will interpret the formula to suggest that roughly 1% of the oxygen lattice sites in the congruent crystal are vacant. In order to have a significant effect on the ionic conductivity in this case, a change in the oxygen vacancy concentration would have to be of this order of magnitude.

We attempted to grow crystals with large alterations in their oxygen vacancy concentrations by the following strategem: crystals were grown from melts consisting of *stoichiometric* $LiNbO_3$ to which was added about 6% of TiO_2 in one case and WO_3 in another. It was hoped that the TiO_2 or WO_3 would replaced the missing Nb_2O_5 in the congruent composition so that the mixed crystals could be grown from an approximately congruent melt. The desired crystalline compositions can be written as $Li_{0.94}[Nb_{0.94}Ti_{0.06}]O_{2.94}$ or $Li_{0.94}[Nb_{0.94}W_{0.06}]O_3$. In other words, the Ti would facilitate the formation of additional oxygen vacancies, and W would suppress oxygen vacancies in numbers comparable to the total population of oxygen vacancies.

Crystals grown from melts with these compositions, like the heavily Si-doped crystals, contained numerous strings of gas inclusions running in the growth direction. There were, however, sufficiently large, clear areas to permit holograms to be stored in the crystals.

Mg was routinely incorporated in $LiNbO_3$ in the early days of research on this material. The distribution coefficient is estimated to be at least 0.5.

10

We grew one crystal from a melt containing 0.5% Mg, 0.05% Fe. The composition of the crystal was checked by emission spectroscopy and found to be sufficiently close to the melt composition for our purposes. Quantitative analysis for Mg was not attempted.

III. FIXING RATE INVESTIGATIONS

Holograms are fixed in $LiNbO_3$ crystals via the thermally activated drift of an ionic species in the electric field of the trapped electronic space-charge pattern. The time required to compensate the field of the electronic space-charge pattern is the dielectric relaxation time τ

$$\tau = \epsilon/\sigma \tag{1}$$

where ϵ is the static dielectric constant and σ is the conductivity attributable to the ionic motion. (We neglect here electronic contributions to the charge screening process.) At a given temperature the rate at which the trapped electronic space-charge field and, thus, diffraction efficiency of the hologram increases is determined by the incident laser power, crystal absorption, etc., while the rate at which this field is compensated is τ^{-1}. Thus the hologram diffraction efficiency will increase during exposure to the recording beams and subsequently decrease after one of the recording beams is removed. The diffraction efficiency η as a function of time τ during this latter period is for small diffraction efficiencies (neglecting thermal and optical erasure)

$$\eta = \sin^2 \beta E = \sin^2 \beta E_o e^{-t/\tau} \approx \beta^2 E_o^2 e^{-2t/\tau} \tag{2}$$

where β is a constant, E is the instantaneous net space-charge field, and E_o is the initial net space-charge field. Therefore, by monitoring the decrease in the diffraction efficiency and assuming that electronic conductivity makes a negligible contribution, we can directly measure the conductivity due to the species responsible for the fixing of holograms. In this section we present measurements of the fixing time and the activation energy for these processes using this technique.

A. MEASUREMENT TECHNIQUES

The measurements were made using the holographic recording apparatus shown schematically in Fig. 2. Holograms were recorded to a diffraction efficiency of ~10%, both recording beams were shut off, and the diffraction efficiency as a function of time was then monitored by periodically turning the reference beam on. This latter procedure was followed to reduce optical erasure.

12

Figure 2. Schematic diagram of the holographic recording apparatus.

Erasure of the electronic space-charge pattern via thermal ionization of the trapped charge has been shown to have an activation energy of ~ 1.48 eV [8] as compared with 1.1 to 1.2 eV for the fixing process [2], and is unimportant over the measuring times used here. To monitor the hologram decay, the photodetector output is displayed on the ordinate axis of an X-Y recorder, and the abscissa is driven by an internal time drive. For fixing times less than several seconds, the hologram is read out continuously and the readout light intensity is displayed on a Tektronix Model 589 storage oscilloscope as a function of time. The trace was photographed and the decay time measured from the photograph. Using this latter technique, decay times on the order of 0.2 s could be measured. This approach was used to measure fast fixing crystals in the temperature range of interest and to extend the measurements into the temperature range covered by the conductivity measurements.

B. STUDIES OF Si-DOPED CRYSTALS

1. Diffusion-Doped Crystals

Si was added to two crystals, one containing 0.02 mole % Fe, and the second containing 0.1 mole % Fe, by diffusion as discussed in Section II.C.

8. D. L. Staebler, W. J. Burke, W. Phillips, and J. J. Amodei, Appl. Phys. Letters 26, 182 (1975).
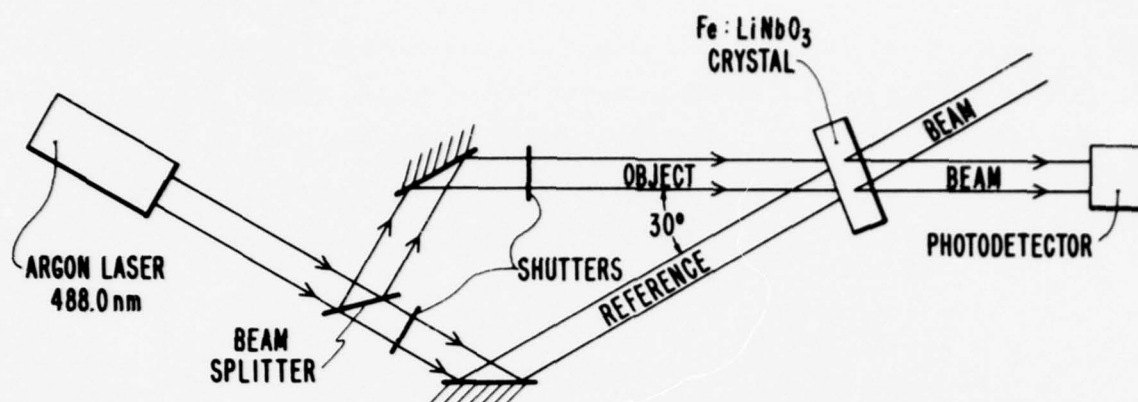
13

Figure 2. Schematic diagram of the holographic recording apparatus.

Erasure of the electronic space-charge pattern via thermal ionization of the trapped charge has been shown to have an activation energy of ~ 1.48 eV [8] as compared with 1.1 to 1.2 eV for the fixing process [2], and is unimportant over the measuring times used here. To monitor the hologram decay, the photodetector output is displayed on the ordinate axis of an X-Y recorder, and the abscissa is driven by an internal time drive. For fixing times less than several seconds, the hologram is read out continuously and the readout light intensity is displayed on a Tektronix Model 589 storage oscilloscope as a function of time. The trace was photographed and the decay time measured from the photograph. Using this latter technique, decay times on the order of 0.2 s could be measured. This approach was used to measure fast fixing crystals in the temperature range of interest and to extend the measurements into the temperature range covered by the conductivity measurements.

B.   STUDIES OF Si-DOPED CRYSTALS

1.   Diffusion-Doped Crystals

Si was added to two crystals, one containing 0.02 mole % Fe, and the second containing 0.1 mole % Fe, by diffusion as discussed in Section II.C.

8.   D. L. Staebler, W. J. Burke, W. Phillips, and J. J. Amodei, Appl. Phys. Letters 26, 182 (1975).

13

The results for the 0.02 and 0.1 mole % crystals are shown in Figs. 3 and 4. The 0.02 mole % crystal showed a slight increase in the fixing time while the 0.1 mole % crystal showed a 50% increase in the fixing time. The difference between the two samples is within the random variations that we have observed in these measurements.
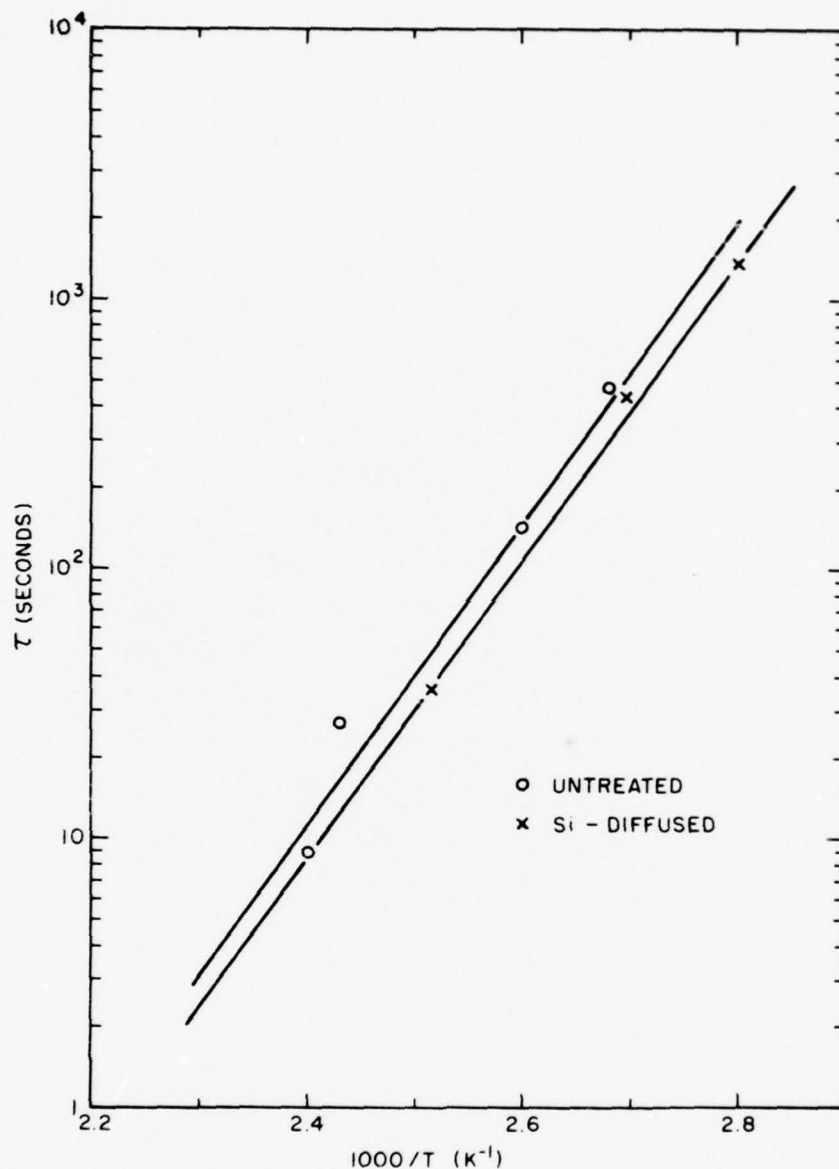
Figure 3. Measured fixing times plotted vs 1000/T for an untreated crystal and a crystal to which Si was added by diffusion, both containing 0.02 mole % Fe.
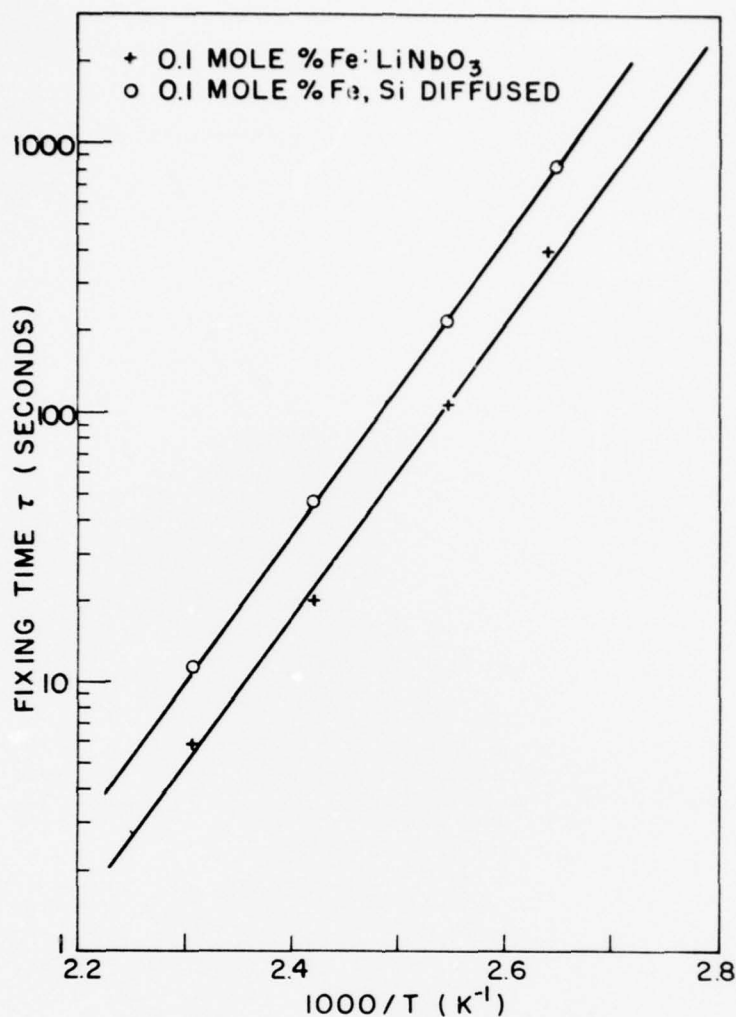
Figure 4. Measured fixing times plotted vs 1000/T for a 0.1 mole % Fe-
doped crystal and a similar crystal into which an attempt
was made to diffuse Si.

2. Crystals Doped With Si During Growth

A total of seven different crystals were grown from Si-doped melts.
Pertinent data for these crystals are summarized in Table 1 (see p. 8). The
Si concentrations in the melts were varied from 0.003 mole % to 1.0 mole %
while the Fe concentration was held to 0.05 mole % for all but two of the
crystals. The concentrations of Si found in the crystals by emission spectro-
scopy were equal to or below the background level of the Si assays for all but
three crystals. The latter were grown from melts containing 0.5 or 1 mole %

15

Si and, as discussed earlier, there is an anomaly in the amount of Si actually incorporated into the crystal (see Table 1).
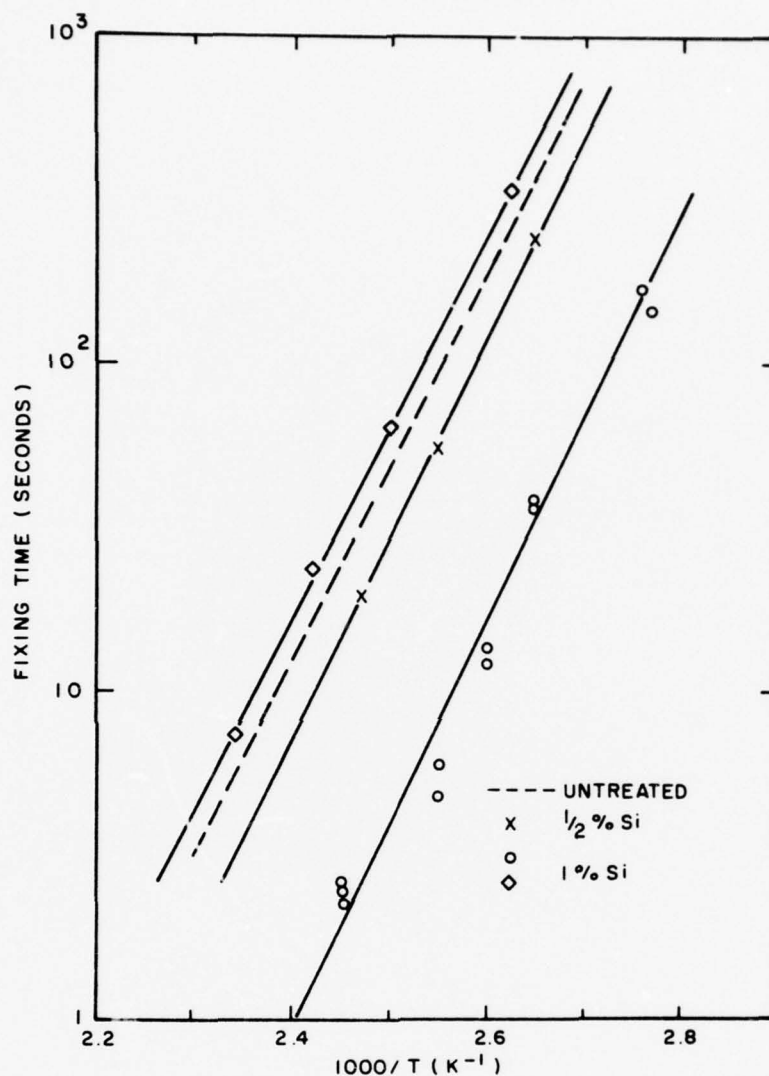
Figure 5. Measured fixing times plotted vs 1000/T for an untreated crystal, a 0.5 mole % Si-doped crystal, and two 1 mole % Si-doped crystals.

Fixing times measured for samples cut from the above three crystals are shown in Fig. 5. Also shown is a typical curve for a cystal containing Fe but no Si. These results show that for the 0.5% and one of the 1% (containing ∿70 ppm of Si) crystals no significant change in the fixing times was observed. The second 1 mole % Si-doped crystal (containing ∿250 ppm of Si)

16

showed a significant decrease in the fixing times. This change is much larger than is typically found between boules and corresponds to the shortest fixing times which we have ever observed in LiNbO$_3$ crystal.

C. OTHER DOPANTS

1. Excess Li

Crystals taken from boules containing 0.02 mole % and 0.002 mole % Fe were annealed in Li$_2$CO$_3$ powder to incorporate interstitial Li. The results obtained for the 0.02% crystal are shown in Fig. 6. In each case, a small decrease in the fixing time was measured, but the decrease is within the range of random variations.

2. Mg Doping

A Mg-doped LiNbO$_3$:Fe crystal was obtained by growth from a melt containing 0.5 mole % Mg and 0.057 mole % Fe. The fixing time for this crystal is shown in Fig. 7. The dashed line in Fig. 7 is a typical curve for the fixing time in a crystal containing Fe only. The fixing time of the Mg-doped crystal is larger by roughly a factor of two than the Fe-only crystal; however, this is not outside the normal range of variation.

3. Ti Doping

A Ti-doped crystal was grown to check the possibility that oxygen vacancies (introduced as charge compensators to the Ti ions) are a major participant in the fixing process. The fixing rate for this crystal did not differ from normal crystals. This could mean that the doping failed to induce the anticipated additional vacancies or that these vacancies do not participate in the fixing to a measurable extent. The behavior of the ionic conductivity with temperature suggests that the former is indeed correct.

4. W Doping

Crystals were prepared from a boule grown from a melt containing 6 mole % W in addition to Fe. W, which is incorporated in LiNbO$_3$ in the 6+ valence state, will reduce the oxygen vacancy concentration to maintain charge compensation. There was no significant difference in either the fixing times or the

17
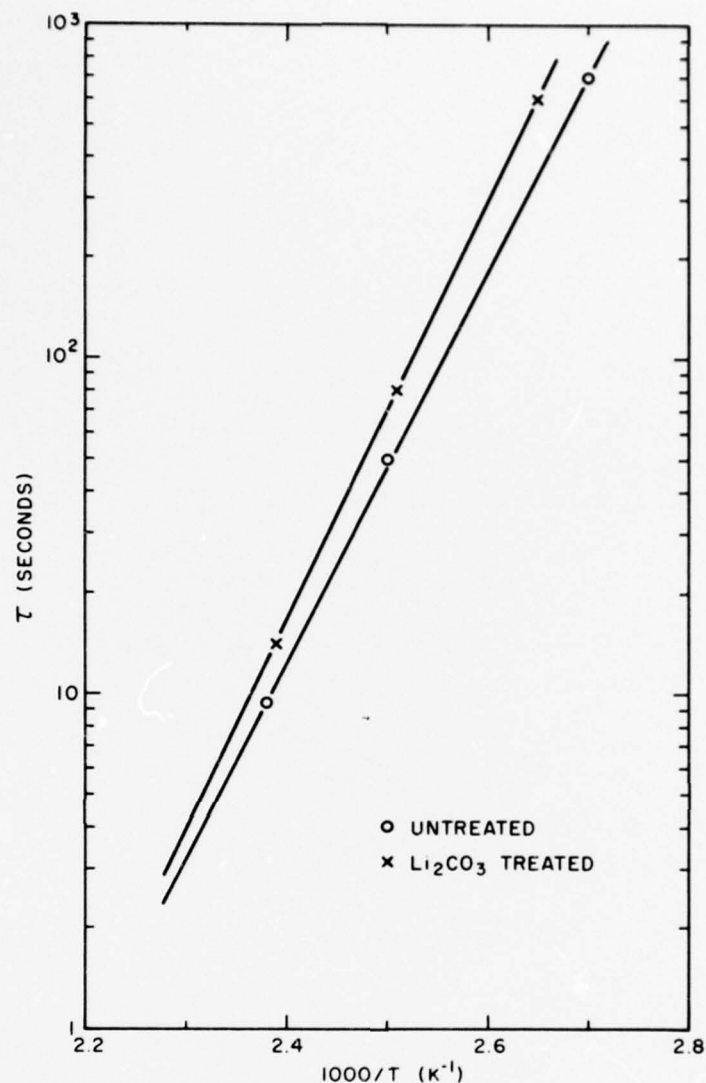
Figure 6. Measured fixing times plotted vs 1000/T for a 0.02 mole %
Fe-doped crystal and a similar crystal annealed in Li_2CO_3
for 120 hours at 585°C. The crystals were Ar-O_2 annealed
to produce the same Fe^{2+} concentration in each.

activation energy for the fixing process as compared with crystals containing
Fe only and grown from the same starting materials.

D. SUMMARY OF FIXING MEASUREMENTS

    The result of the fixing measurements can be summarized as follows: With
the exception of crystal 03244, none of the crystals studied differed in

18
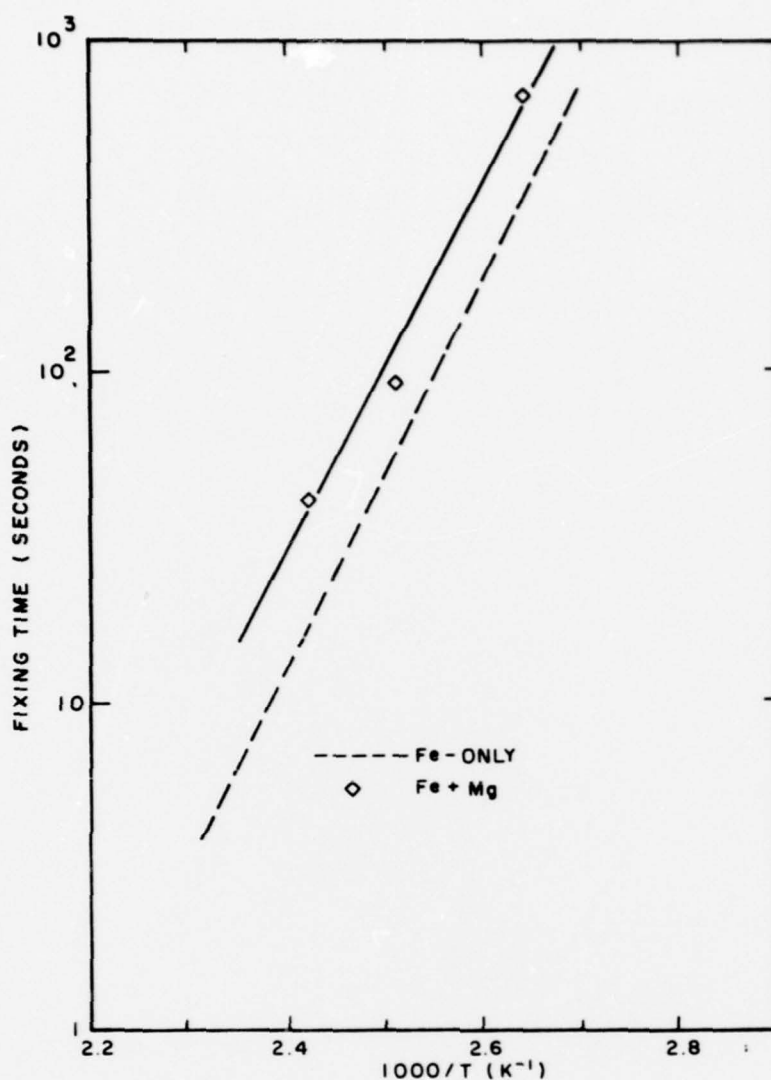
Figure 7. Measured fixing time plotted vs 1000/T for crystal containing Fe only and crystal containing 0.057 mole % Fe plus 0.5 mole % Fe plus 0.5 mole % Mg.

fixing rate from normal crystals by more than the random variation that has been observed in normal crystals. Crystal 03244 contained the largest amount of Si and exhibited the fastest fixing time ever observed in $LiNbO_3$:Fe. However, other crystals containing elevated amounts of Si did not show significant changes in fixing time. This can be interpreted to suggest that Si can indeed play a role in the fixing process when it is present in large quantities, but

19

the effect is apparently masked at low Si concentrations by other unknown ionic processes.

IV. IONIC CONDUCTIVITY

This section describes research on the ionic conductivity of $LiNbO_3$. The aim here was to help identify the mobile ionic species responsible for fixing. Nearly all the crystals studied were doped with two types of impurities. One of them (Fe) was needed to sensitize the material for hologram storage. The other dopant was added in an attempt to change the ionic conductivity, either directly (through motion of the impurity itself) or indirectly (through charge-compensating changes in the concentration of mobile intrinsic defects). The main thrust of this work was centered on Si ions because preliminary results [3] strongly suggested that they are mobile at the temperatures used for fixing. Our results, in conjunction with the fixing measurements discussed previously, indicated that Si could indeed be involved, but other ionic defects probably dominate the conductivity. The net result is that no consistent means has been found for tailoring the ionic conductivity

A. EXPERIMENTAL METHODS

All experiments were carried out on cut and polished samples heated on a hot plate. Voltage was applied with a Kepco power supply (BHK 2000-0.1M), and the current measured with a Keithly 610A electrometer. Contacts were DAG (colloidal graphite) applied to opposite faces of the sample. In all cases, ohmic behavior was verified by measuring the current for at least two different applied voltages to ensure that contact problems were not interfering with the experiment. Electro-optic experiments confirmed this by allowing us to directly measure the applied electric field [9]. An additional conductivity experiment with samples of various geometries established that only bulk properties were being measured [10].

9. W. Phillips, W. J. Burke, and D. L. Staebler, *Materials for Volume Phase Holography*, Quarterly Report No. 2 prepared for Naval Air Systems Command for Contract No. N00019-76-C-0116, May 1976.
10. W. J. Burke, W. Phillips, and D. L. Staebler, *Materials for Volume Phase Holography*, Quarterly Report No.1 prepared for Naval Air Systems Command under Contract No. N00019-76-C-0116, February 1976.

B. VARIATIONS IN CONDUCTIVITY

When our research began on $LiNbO_3$ more than 5 years ago, we noticed that the ionic conductivity could vary over a range of about a factor of four from sample to sample without any apparent correlation with dopant or sample history. Figure 8 shows some data from that early work [2]. It is plotted on a scale chosen to find the activation energy (E_a) for the conductivity, assuming the relation

$$\sigma = \sigma_o \exp(-E_a/kT) \tag{3}$$

where σ is the conductivity, σ_o is a constant, k is Boltzmann's constant, and T is the temperature. Both σ and E_a varied from sample to sample, but not enough to suggest that the impurity level or sample origin had an important influence. Thus we directed our attention to more pressing issues such as the problems of multiple storage [8] and scattering due to optically induced inhomogeneities [1]. Because of our success in those areas, and because of our continued interest in improving the performance of Fe-doped $LiNbO_3$, we returned to the question of sample variability in conductivity. We concentrated this time on the samples particularly useful for fixing applications, lightly reduced crystals of $LiNbO_3$ doped with relatively high concentrations (>0.02%) of Fe. Figure 9 shows two of the most extreme cases that we found. The lower doped sample is similar to those studied before; in particular it agrees quite well with the 0.05% Fe data of Fig. 8. The more heavily doped sample also falls in the conductivity range of Fig. 8, but has a higher activation energy. This suggests that a different mechanism (or defect) is involved in the conductivity process. Thus, although the variation of the Fe doping level in itself has little effect on the magnitude of the conductivity, it does seem to change the mechanism. Apparently the conductivity processes are more complex than we had thought. In particular, it seems unlikely that a single species of ionic defect is responsible for the fixing in Fe-doped $LiNbO_3$.

C. EFFECT OF CODOPING

A number of crystals doped with another impurity (in addition to Fe) were tested. Most of these were Fe-Si doped, and some representative results

22
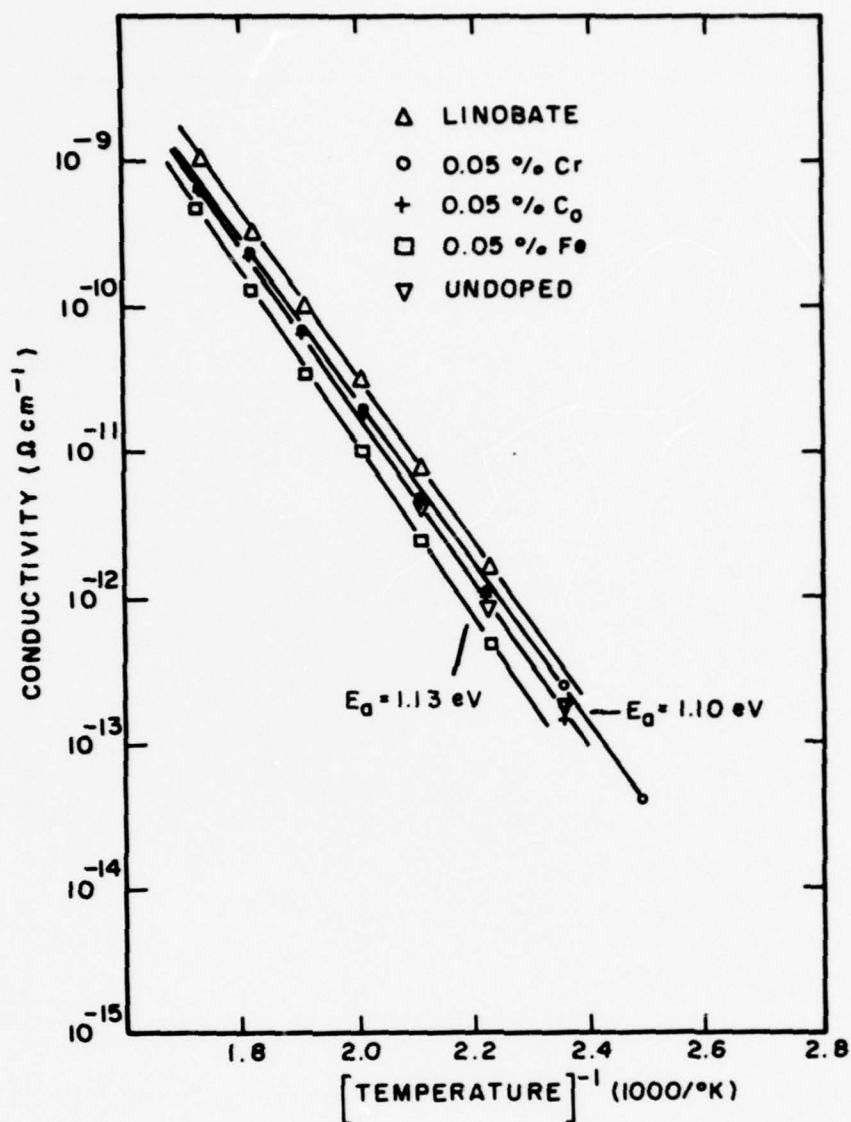
Figure 8. Conductivity as a function of temperature for a number of samples grown by RCA Laboratories, plus an undoped "linobate" sample purchased from Crystal Technology. E_a is the activation energy (from early studies published in Ref. 2).
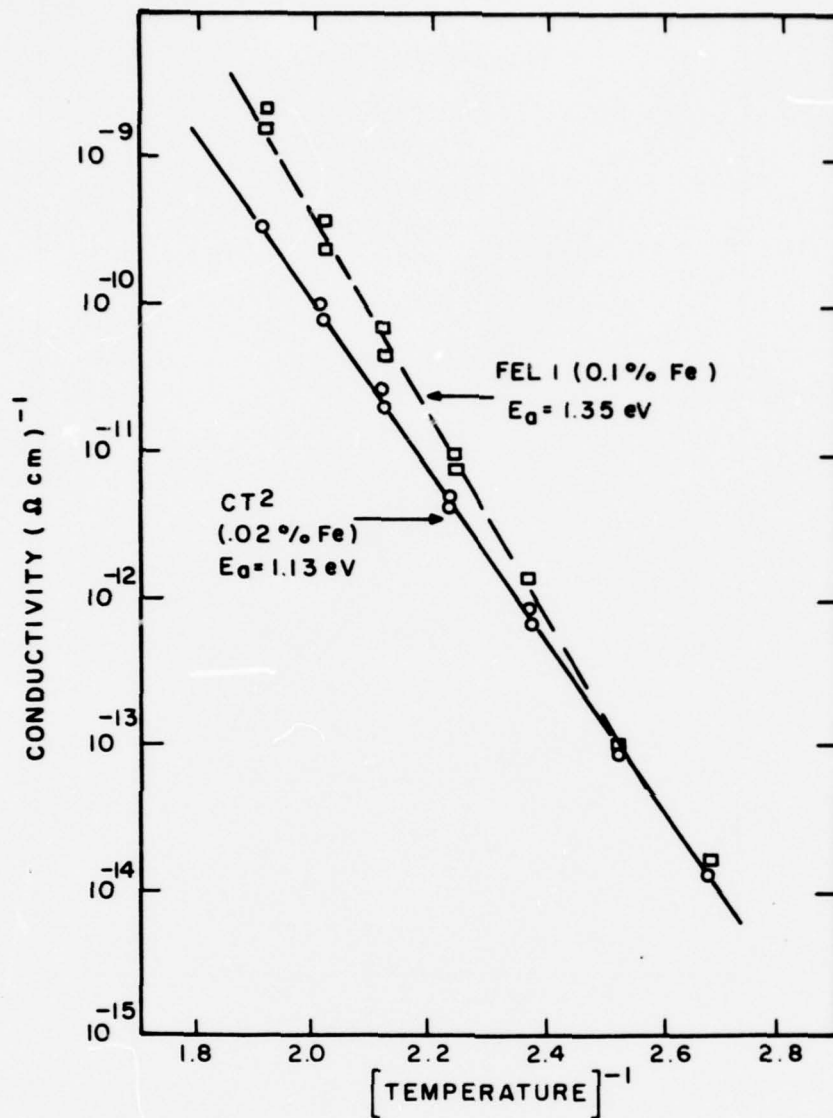
Figure 9. Conductivity curves showing the range in acti-
vation energy found in Fe-doped crystals.

for these are shown in Figure 10. In general, they fall within the range
of conductivity established by Fig. 8, with the single exception of one of
the 1% Si-doped samples; its conductivity was slightly higher. Nevertheless,
the increase is not very large, particularly in the temperature range used
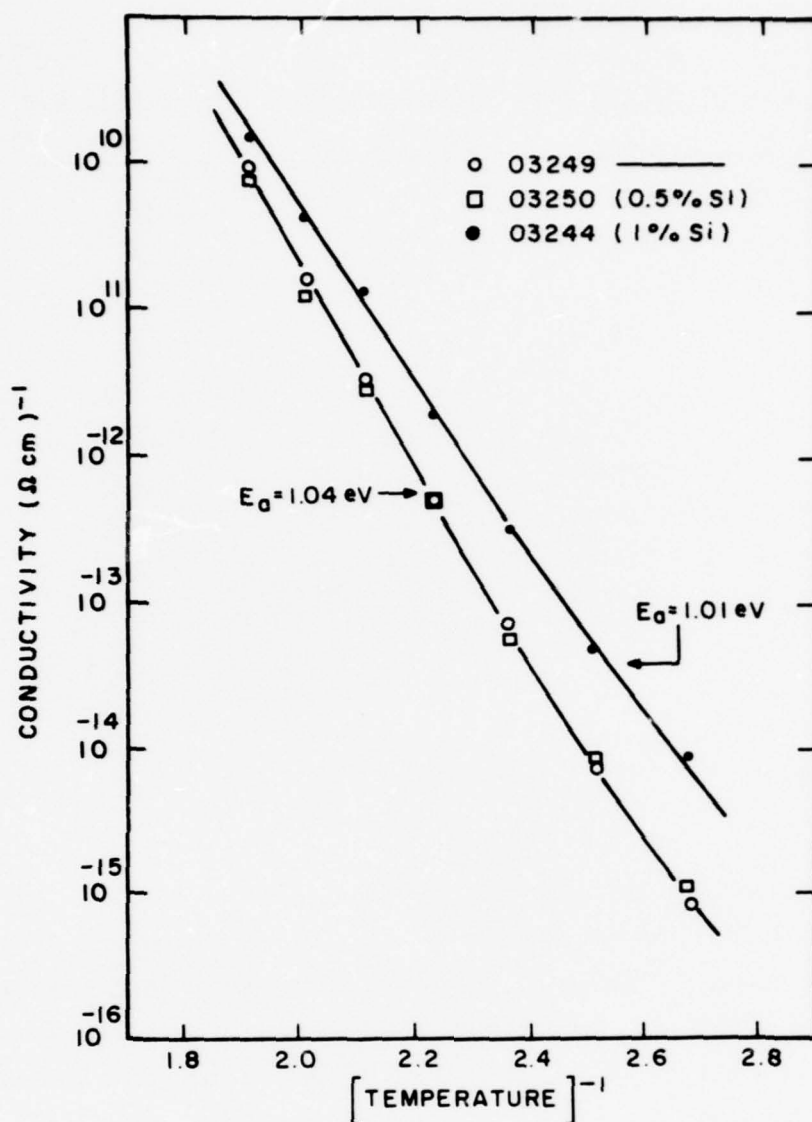
Figure 10. Conductivity of several Si-doped samples, and one without Si. All contain 0.05% Fe. The change in slope around $1/T = 2.4 \times 10^{-3}$ is discussed in the text.

for fixing ($\sim 160°$ to $140°C$). Table 3 shows the conductivity at $144°C$ for the samples studied during this program. It is clear that if Si doping indeed has an effect, it is fairly small, a factor of two or less. Table 3 also shows the time constants for fixing. The measured values were taken from

TABLE 3. EFFECTS OF CODOPING

	Nominal Doping (%)		Conductivity	τ calculated	τ measured
Sample	Fe	Si	$10^{-14}(\Omega\ cm)^{-1}$	(s)	(s)
03231	0.05	0.033	5	25	5
03239	0.05	0.1	6	21	7
03244	0.05	1	25	5	1
03250	0.05	0.5	4	31	7
03256	0.05	1	5	25	17
FEL 1	0.1	–	8	15	20
FEL 1	0.1	Si-diffused	8	15	31
	0.02	Si-diffused	3	41	9
	0.02	Li-diffused	3	41	17
03242	0.03	6 % Ti	7	18	25
Linobate	–	–	17	7	6

Note – all values are for T = 144°C

the results in Section III and from previous reports [8,9,10]. The others were calculated from the conductivity, using the fixing model equations (1) and (2). The agreement is good. The scatter is due probably to inaccuracies in the applied field (due to fringing effects) and slight variations in the sample temperature. It is interesting to note that the best sample (i.e., the one with the shortest fixing time) is 03244 (doped with 1% Si), and this is true for both the calculated and measured values.

D. ACTIVATION ENERGY

A new result of our work, not previously seen in Fe-doped $LiNbO_3$, was the observation of a distinct change in the activation energy with temperature. Figure 10 shows this most clearly. Below ∿150°C, the activation energy is as low as 1 eV; above ∿150°C it is higher, with ∿1.35 eV the highest found thus far. This behavior accounts for the discrepancy that we

26

previously observed between the activation energies measured by different techniques. The conductivity measurements were usually carried out in the higher temperature range, and thus found a higher activation energy than that determined from the fixing measurement at lower temperatures.

The reason for this variation in activation energy with temperature is not clear. It is not directly related to Si content, as shown by sample 03249 in Fig. 10, and to a lesser extent by sample FEL 1; neither were doped with Si but show the change in E_a. In addition, it is quite noticeable in the Li-diffused sample [11]. The most likely reason is that more than one species of ionic defects are involved in the conductivity, as proposed in section B above. (A similar model has been, in fact, used by Bollman and Gernand [12] to describe the conductivity in undoped $LiNbO_3$ at elevated temperatures.) The activation energy then depends on the relative concentrations and mobilities of the species contributing to the ionic conductivity which in turn depends on the temperature.

In this model, an activation energy change, like that shown in Figure 10, will occur at the temperature at which the relative effects of the two species are equal. Above this temperature the high activation energy species will predominate because it is the one influenced more by temperature changes. Below this temperature, the lower activation energy species take over. The appearance of this behavior in some of our crystals and not others is puzzling. It could be due to charge compensation effects. To check this, a sample was doped with 6% Ti in an effort to increase the concentration of oxygen vacancies (see Section III.C.3 above). This sample also showed the changeover at $\sim150°C$ indicating that the dopant had no effect on the concentration of oxygen vacancies. Whatever the reason for these effects, it seems clear that one cannot easily tailor the conductivity in the temperature range used for fixing.

11. W. Phillips, W. J. Burke, and D. L. Staebler, *Materials for Volume Phase Holography*, Quarterly Report No. 3 prepared for Naval Air Systems Command under Contract No. N00019-76-C-0116, August 1976.
12. W. Bollman and N. Gernand, Phys. Stat. Sol. (a) 9. 301 (1972).

27

V. CONCLUSIONS

Of the many strategies by which we tried to influence the ionic conductivity and the fixing rate of LiNbO$_3$:Fe, only heavy Si doping produced an effect that was larger than the random variations observed in these quantities. The effect of the Si doping was not reproduced in a second crystal, but this can be attributed to our inability to achieve the same doping level as the first crystal. These results can be interpreted as suggesting that Si is mobile under some conditions at the fixing temperature, but that its effects are masked by more abundant charge carriers at all but very high concentrations. Other interpretations are possible, but this seems to be the most economical way of interpreting the results we have accumulated.

Of practical significance is the extremely low optical quality of the crystals containing measurable amounts of Si. It appears that even if we could incorporate enough Si to reproduce the results of the heavily doped crystal, the problems of obtaining acceptable optical quality would be enormous.

For this reason it is our judgment that at the present time, information storage and retrieval systems based on fixed holograms in LiNbO$_3$:Fe should make use of high optical quality, singly doped material. Any gains that might be made through Si doping would be offset by the deterioration of the optical quality of the storage medium.

PART 2

CAPABILITIES OF INFORMATION STORAGE/RETRIEVAL SYSTEMS BASED ON $LiNbO_3$:Fe

The purpose of the extended 5-year program described in this report has been to develop a volume holographic image storage system, one potential application of which is in the Navy's moving map display program. Volume holograms are of interest in the map display program because of their capability for high resolution and high density storage of information coupled with the ease of access of individual holograms. The volume holographic storage system has three basic components: the storage medium, the accessing system, and the image display device. In Part 2 of the report we review the results of the studies of a volume holographic storage system for the moving map display program made at RCA Laboratories with Navy support. The primary emphasis of our effort has been on the development of the storage medium itself, since this is the key element of the system and did not exist at the start of this program.

In the first portion of Part 2 we summarize the properties of the storage medium that are relevant to the ultimate capabilities of the system, such as sensitivity, dynamic range, storage capacity and the like. In the second portion we discuss systems considerations relevant to the moving map display application.

I.   HOLOGRAPHIC PROPERTIES OF $LiNbO_3$:Fe

A.   SENSITIVITY

The diffraction efficiency produced by a given exposure from the interfering laser beams is a measure of the sensitivity. It depends on both the charge transport and electro-optic properties of the particular crystal being used. A theoretical approach is given below, and measured values for Fe-doped $LiNbO_3$ follow.

The derivation for the sensitivity follows from the theory of Amodei [13]. The crystal's absorption is taken into account here, and we only consider the

_____

13.   J. J. Amodei, RCA Review 32, 185 (1971).

29

early stage of storage, where the refractive index modulation is linear with exposure. The result holds true only for low diffraction efficiency ($\eta < 40\%$), and is independent of crystal thickness. The sensitivity (S) is defined as

$$S = \eta^{1/2}/E \tag{4}$$

where η is the diffraction efficiency (diffracted intensity/incident readout intensity) and E is It, the product of the power density of the incident storage light (I) and the storage time (t).

First, the expression of Amodei [13] is used to find the magnitude of the space-charge field (E_1) for a given free electron generation rate (G) and storage time (t). This is then related to E from

$$G = 2If/3h\nu d \tag{5}$$

where $h\nu$ is the energy of the absorbed photons, f is the probability that an absorbed photon produces a free carrier, and d is the crystal thickness (an arbitrary parameter that cancels out later).

Next, the refractive index change (Δn) caused by E_1 is found from the electro-optic coefficients of the crystal. This is highly dependent on the orientation of the crystal and is maximum for the orientation usually used in this work. For this case one has [14]:

$$\Delta n = [n_e^3 r_{33}/2]E_1 \tag{6}$$

where n_e is the extraordinary index of refraction and r_{33} is the relevant component of the electro-optic tensor. The diffraction efficiency is now determined from Kogelnik's equation [15], giving

$$S = [m/\cos\theta] \, [A\sqrt{1-A}] \, [fL] \, [n_e^3 r_{33}/2\epsilon] \, [\pi e/hc] \tag{7}$$

The bracketed terms, and their maximum values, are discussed below.

14. See, e.g., *Handbook of Lasers*, R. J. Pressley, Ed. (Chemical Rubber Co., 1971).
15. H. Kogelnik, Bell Syst. Tech. J. 48, 2909 (1969).

The first term depends on the relative intensity and angle (θ) of the beams; $m = 1$ for beams of equal intensity.

The second term reflects the effect of the crystal absorption (A) during storage and transmission (1–A) during readout. The maximum value $(2/3\sqrt{3})$ occurs for $A = 2/3$.

The third term contains L, the distance that an absorbed photon displaces a trapped charge. In the crystals used in this program for multiple storage, storage occurs via the bulk photovoltaic effect, and $L \simeq 1$ Å. The maximum value of f is unity.

The fourth term in brackets reflects the electro-optic and dielectric properties of the particular material being considered. It, however, varies little from material to material [14]. This is because both r_{33} and ε represent the ease with which the material's polarization is affected by an electric field. The last bracketed term is composed of the electronic charge (e), Planck's constant (h), and the velocity of light (c).

Equation (7) is now used to calculate the theoretical sensitivity for Fe-doped $LiNbO_3$. We assume that $A = 2/3$, and that f, m, and $\cos\theta$ are all unity. ($\cos\theta$ is not far from unity in a typical situation, e.g., $\cos\theta = 0.96$ for a 1-µm grating produced by interference of 4880-Å beams.) We also use $n_e = 2.277$, $r_{33} = 3.2 \times 10^{-11}$ m/V, and $\varepsilon_{33} = 2.83 \times 10^{-10}$ F/m. From Eq. (7) we now find that $S \stackrel{\sim}{\sim} 1$ cm^2/J. This means that a diffraction efficiency of $\sim 40\%$ would require slightly less than 1 J/cm^2 of incident light, consistent with experiment.

Higher sensitivities have been achieved in heavily reduced, lightly doped crystals, primarily because L in Eq. (7) is increased by the much smaller density of empty traps. Holograms cannot be fixed, however, in these samples, and their multiple storage capacity is quite low because of their high erase sensitivity. These crystals are best suited for read/write applications. For the read/only archival applications of importance to this program, only the heavily doped, lightly reduced crystals can be used, and the sensitivity of these crystals is limited by a small L [~ 1 Å in Eq. (7)].

The sensitivity for storage of fixed holograms is somewhat lower than that discussed above because the fixing process, although quite permanent, is not 100% effective; a significant fraction of the recorded ionic space charge is

screened out during readout. As a result, about 5 J/cm^2 of incident light is required to record a fixed hologram with a diffraction efficiency of ∿40% [8].

B. DYNAMIC RANGE

The dynamic range of a phase storage medium is its maximum possible photo-induced change of the refractive index. It determines the largest diffraction efficiency that can be recorded in a crystal of a given thickness and the number of different holograms that can be recorded in a given volume.

There are two theoretical limits to the dynamic range in LiNbO$_3$. The first is the density of empty or occupied traps, whichever is lower. This determines the largest space-charge density that can be built up during exposure to light. Assuming sinusoidal gratings, one can show that the charge density required for a given index is inversely proportional to the grating spacing. For a 1-μm grating spacing, an index change of 2×10^{-5} is produced with a trap density of only 10^{15} cm^{-3}. Fe-doped crystals used for fixing do not normally have a problem in this respect because the trap concentrations are in excess of 10^{18} cm^{-3}. Read/write crystals, however, can be limited. These are low doped crystals that are heavily reduced so as to have a very low density of empty traps. This situation enhances the erasure sensitivity but at the expense of a limited storage range [16].

The second limitation on the dynamic range is the equilibrium space-charge field. It saturates when the field of the hologram has become comparable to the effective field for storage. If diffusion is the dominant process, the equilibrium field is given simply by the effective field for diffusion, $E_D = (2\pi/\ell)(kT/e)$. For a grating spacing (ℓ) of ∿1 μm and a temperature (T) of 300°K, this is ∿1.6 kV/cm. The maximum index change (Δn) is then determined by the electro-optic coefficient of the material being used. For LiNbO$_3$, Δn is 3×10^{-5}.

The largest possible index charge occurs when storage occurs via a uniform electric field. In LiNbO$_3$ an equivalent field is generated internally via the bulk photovoltaic effect. The largest field is ∿10^5 kV/cm giving ∿2×10^{-3} as the maximum index change, consistent with measured values.

---

16. D. L. Staebler and W. Phillips, Appl. Optics 13, 789 (1974).

Holograms fixed in $LiNbO_3$ have a smaller dynamic range ($\sim 4 \times 10^{-4}$) due to partial compensation of the ionic space charge.

A large dynamic range allows the use of thin crystals (e.g., ~ 10 μm) for hologram storage, but it is not necessary for thicker crystals unless one is interested in multiple storage. The storage capacity of crystals used in multiple storage applications is discussed below.

C. STORAGE CAPACITY

We consider here a thick crystal in which a large number of holograms are sequentially recorded, each one at a slightly different angle. This scheme is practical only for fixed holograms. If they are not fixed, continued readout of one hologram would erase the others. The primary limit on capacity is the angular resolution of the hologram readout. The bandwidth for readout is given (in radians) by $\sim \ell/d$, the ratio of the grating spacing to the sample thickness. Assuming an ℓ of 1 μm, d of 1 cm, and an available angular spread of one radian ($\sim 57°$), the maximum capacity is 10^4 holograms. A more practical consideration of hologram overlap problems reduces this to $\sim 10^3$ holograms.

The other limitations on storage capacity involve a tradeoff with diffraction efficiency. Here the minimum signal-to-noise ratio that a given application can tolerate becomes important. One limitation is the dynamic range. If it is very small, the sample's recording range is exhausted by only a few holograms, and further storage distorts the previously recorded patterns. An analytical treatment of this problem and its effect on the signal-to-noise ratio has not been carried out. Nevertheless, one can make a "worst case" analysis to find the point at which no degradation of any kind will occur. This is when the sum of the index changes of the holograms equals the recording range. From this one finds (for a 1-cm crystal and 500.0-nm light)

$$\eta = 2 \times 10^9 \ (\Delta n/N)^2 \tag{8}$$

where N is the number of the holograms, each one with an index change of Δn, and efficiency η. Using the values discussed above ($\Delta n \stackrel{\sim}{\sim} 4 \times 10^{-4}$, $N = 10^3$) we find $\eta = 0.03\%$. Our experience shows that this is an extremely conservative calculation; much higher efficiencies are possible for 10^3 holograms.

33

The other limitation is erasure during storage. Although the "write-while-hot" technique stores fixed holograms, there is some erasure at the elevated temperature. The important parameter here is β, the ratio of the erasure time to the storage time. If $\beta \sim 1$, then multiple storage would be quite difficult. The first hologram would be erased during the storage of the second. If $\beta \gg 10^3$, then even storage of 10^3 holograms should not be any problem. We find that $\beta \sim 100$ for most heavily doped, lightly reduced crystals. Thus, erasure has an influence, but by correct recording procedures, it can be compensated. Our best experimental result is 500 fixed holograms, each with more than 2.5% diffraction efficiency [8].

Erasure during storage is due to thermal or optical excitation of trapped electrons. When they diffuse, they pull ionic defects with them. The net result, if allowed to continue, is the complete erasure of both patterns, ionic and electronic. Erasure can be reduced to some extent by material treatment that increases the density of empty traps, which in turn decreases the diffusion length of electrons, making it harder for them to redistribute. In addition, the thermal part of erasure can be reduced by simply storing the holograms at lower temperature. This approach, however, introduces noise and distortions that will be discussed in a later section. Samples with higher ionic conductivity could be important here, but as we discuss in Part 1 of this report such control is not available.

D. RESOLUTION

Since, for the most part, these materials are single crystals, the spatial resolution is in principle limited only by the distance between traps. Consider a trap density of 10^{15} cm^{-3}, the minimum value required for an index change of 2×10^{-5} at a $\sim$1-μm grating spacing. The distance between traps is, on the average, only 1000 $\overset{\circ}{A}$, an order of magnitude smaller than the grating spacing. Thus, the hologram can clearly be recorded at this spatial frequency, but it may have some scattering noise due to statistical fluctuations of the trapped electrons (see subsection F below). The noise would be even more severe at smaller grating spacings. To compound the problem, a smaller grating spacing would lead to a lower refractive index change, assuming a trap-limited situation. For these reasons doping level is quite important. Concentrations

34

in excess of 10^{18} cm^{-3} are used in Fe-doped LiNbO$_3$, giving a distance between traps of only 100 Å.

E. STORAGE TIME

The room temperature storage time of a hologram in Fe-doped LiNbO$_3$ is determined by the dark conductivity of the material. Most crystal materials have low conductivity at room temperatures [$\sim 10^{-18}(\Omega$-cm)$^{-1}$], and this gives storage times of a few months.

It should be noted, however, that the decay of a hologram's diffraction efficiency does not necessarily mean that the information is lost. The dark conductivity is primarily ionic. The decay corresponds in fact to the first step of the fixing process - the formation of an ionic pattern that neutralizes the electronic pattern of the stored hologram. Actual loss of the information occurs only upon thermal activation and subsequent redistribution of the trapped electrons. This process can be quite slow; storage times for fixed holograms of up to 10^5 years are predicted for LiNbO$_3$ [8]. Four years ago, we stored high-quality images in an Fe-doped LiNbO$_3$ crystal. These holograms have been read periodically (monthly) with no degradation.

F. NOISE AND DISTORTION

Since LiNbO$_3$:Fe has no latency, i.e., the refractive index appears immediately upon exposure, certain beam coupling effects that can usually be ignored during recording in latent image media (i.e., photograph film) become quite significant. In principle, a phase hologram can act as a periodic array that couples the two interfering beams that record the holograms. This rearranges their amplitude and phase as they travel through the crystal. The result is to limit or distort the hologram that is ultimately recorded. The analysis of this process has been carried out for the storage of sinusoidal gratings [18,19,20]. A similar effect occurs during optical readout [18,16,20]

17. G. A. Alphonse and W. Phillips, RCA Review 37, 184 (1976).
18. D. L. Staebler and J. J. Amodei, J. Appl. Phys. 43, 1042 (1972).
19. R. Parsons, W. D. Cornish, and L. Young, Appl. Phys. Letters 27, 654 (1975).
20. R. Magnusson and T. K. Gaylord, J. Appl. Phys. 47, 190 (1976).

even of fixed holograms [2]. Although it has not been studied with holograms
that contain information, one suspects that it will limit the useful diffrac-
tion efficiency; holograms with low diffraction efficiency produce little
coupling.

Another problem associated with the lack of latency is the buildup of
optical scattering [21,22]. This occurs when any photosensitive ferroelectric
crystal is exposed to a coherent beam of light. A defect that scatters light
produces a spherical wave that then interferes with the original beam. The
resulting interference patterns are recorded as index changes that, in turn,
lead to more scattering. The result is a rapid buildup of complicated scatter-
ing patterns that produce noise in the readout image. This process occurs
during storage, and thus limits the total exposure (and thus the diffraction
efficiency) that can be used. It also occurs during readout and can be a
particularly severe problem for holograms fixed in highly sensitive materials.

There are means for avoiding the scattering effects. One is to use what
in effect is a latent storage process. Such a process has been demonstrated
in heated crystals of Fe-doped $LiNbO_3$. At a sufficiently high temperature
(e.g., ∿160°C), fixing occurs simultaneously with storage. This limits the
largest index change that can be built up during storage and thus prevents the
buildup of unwanted scattering [8]. The fixed holograms are then "developed"
by cooling the crystal to room temperature and exposing it to light. Another
method to avoid scattering effects, useful for readout, is to render the mate-
rial insensitive to light without disturbing the recorded hologram. This could
be done by applying an electric field antiparallel to the internally generated
field of $LiNbO_3$ [1]. Another approach is to decrease the crystal absorption
after a hologram has been recorded. This has, in fact, been done in photo-
chromic $LiNbO_3$:Fe,Mn [23].

A low dynamic range can also prevent the buildup of scattering. This, of
course, would also result in a low diffraction efficiency unless thick crystals
are used. An important example of the benefit of a low dynamic range is the
read/write materials. These show no buildup of optical scattering during
storage or readout. In fact, the Weiner noise at 1000 lines/mm is only
5×10^{-8}, slightly better than for dichromated gelatin [17].

21. W. Phillips, J. J. Amodei, and D. L. Staebler, RCA Review 33, 94 (1972).
22. R. Magnusson and T. K. Gaylord, Appl. Optics 13, 1545 (1974).
23. D. L. Staebler and W. Phillips, Appl. Phys. Letters 24, 263 (1974).

Optical scattering, if produced, does not prevent use of the crystal. It can be erased. One method is to simply shift the coherent beam (or beams) to a new angle. This erases previously stored scattering, but begins to record more at the new angle. Exposure to incoherent light is a preferrable approach since it erases all spurious optical scattering. This technique has been used to restore the readout quality of fixed holograms in Fe-doped $LiNbO_3$ [8]. Thus, optical induced scattering can be avoided at both stages - with the latency during storage in heated crystals and with erasure by incoherent light during readout.

In addition to spurious optical scattering there are a number of other noise sources in the readout image. These are multiple reflections and optical scattering from defects in the recording and readout optical systems and in the recording medium [24], intermodulation distortion, and crosstalk between holograms stored in the same volume [25]. Each of these noise sources has been investigated during our system development program.

Multiple reflections and optical scattering from defects in the optical systems used for recording and readout and in the recording medium are common to all systems using a highly coherent light source. Multiple reflections from the optical systems can be reduced by the use of antireflection coatings on the optical elements and by aperturing. Reflections from the surfaces of the single-crystal storage medium can also be eliminated by the use of antireflection coatings. We have reduced the reflectivity of $LiNbO_3$ crystals from 20% to 2% by use of a single-layer SiO_2 coating. This coating exhibits excellent stability during repeated heating/cooling cycles typical of those used for the "write-while-hot" recording technique. Further reductions in the crystal reflectivity should be possible with additional effort.

24. W. J. Burke, *S/N Ratio of Holographic Images*, Final Report, Contract No. N00019-75-C-0494, November 1975.
25. W. J. Burke, P. Sheng, and H. A. Weakliem, *Intrinsic Noise Sources in Volume Holography*, Final Report prepared under Contract No. N00014-75-C-0590 for Office of Naval Research, December 1975.

Optical scattering exclusive of that induced by the light beam from bulk and surface defects has been measured to be negligible ($\sim$-100 dB for light scattered from the reconstruction into the readout angle). This is due to the extremely good optical quality of the crystals and to the excellent surface finish obtained.

The dominant noise source is from light scattering in the recording and readout optics. This noise exhibits itself as bullseyes and ring patterns in the readout image. Using redundancy techniques developed for the holotape program [26], we have shown that this noise will be able to be reduced to an acceptable level [24].

Intermodulation distortion, which is a significant limitation on thin phase holograms, is negligible for thick phase holograms ($\sim$1-cm thick) since the magnitude of the effect decreases as $1/d^2$ where d is the thickness of the storage medium. This is because for a given diffraction efficiency the required index of refraction change for a thick phase hologram is much smaller than for a thin phase hologram.

Crosstalk noise arises from the off-Bragg readout of holograms other than the hologram of interest simultaneous with the readout of the hologram of interest. Our studies have shown that with a proper choice of the angular spacing between holograms, a signal-to-noise (s/n) ratio of 40 dB due to crosstalk noise is possible. Figure 11 shows the results of measurements of the s/n ratio made on a 0.826-cm-thick crystal of Fe-doped LiNbO$_3$ in which 50 holograms had been recorded. The oscillations in the s/n ratio are due to the oscillations in the off-Bragg amplitude of the holograms recorded in this thickness crystal. The theoretical curves were calculated for the two cases of coherent and incoherent addition of the off-Bragg amplitudes. The experimental results are roughly midway between these two cases, implying that the scattered amplitudes from the different holograms are only partially coherent. The effective grating thickness required to fit the oscillations in the s/n ratio is less than the actual crystal thickness due to absorption effects in the crystal. Our measurements show that there is no decrease in the s/n ratio with an additional increase in the number of holograms since only those holograms whose

26. A. H. Firester, E. C. Fox, T. Gayeski, W. J. Hannan, and M. Lurie, RCA Review 33, 131 (1972).

angular positions are within ∿3 degrees of the hologram of interest contribute.
As can be seen from Fig. 11, an angular spacing of 0.1 degree between holo-
grams gives a high s/n ratio and is compatible with the storage of >500 holo-
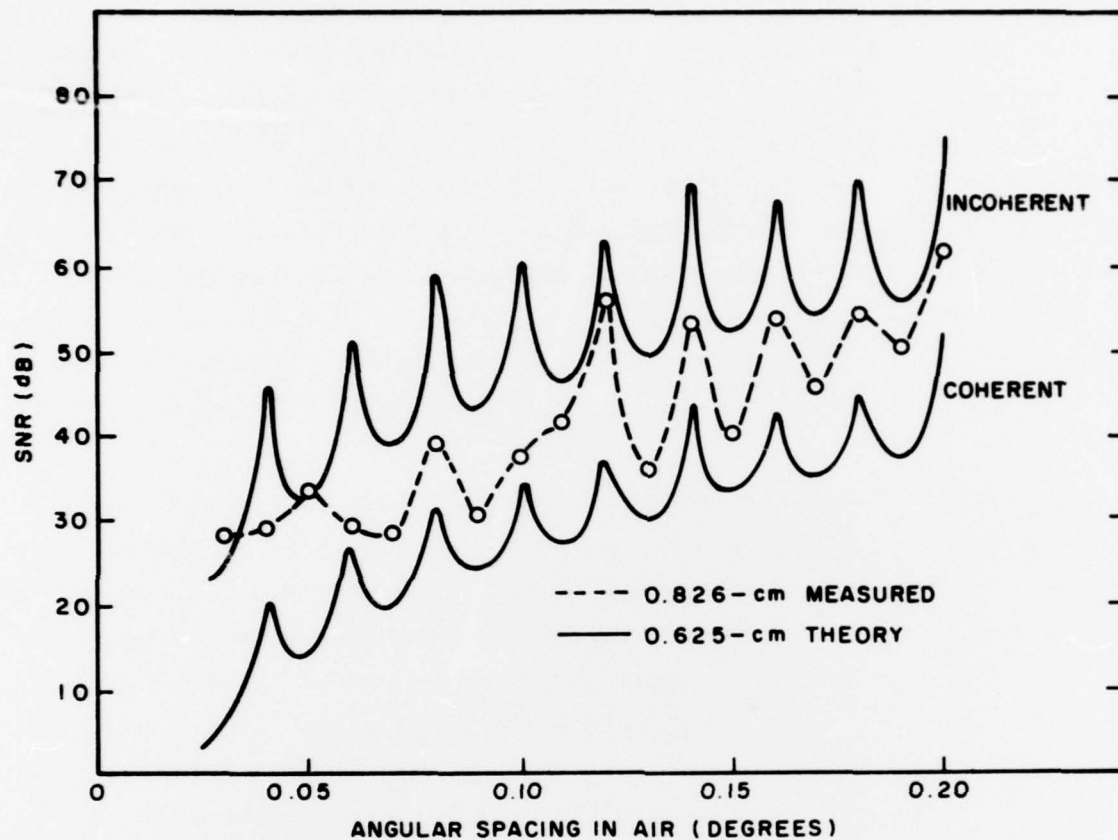grams in a 1-cm-thick crystal.

Figure 11. Signal-to-noise ratio measurements.

II. SYSTEMS CONSIDERATIONS

A. ACCESSING AND RETRIEVAL TECHNIQUES

The angular or wavelength selectivity of holograms stored in a thick phase storage medium allows many holograms to be stored in the same volume; e.g., over 500 holograms have been stored in a 1-cm-thick crystal of Fe-doped $LiNbO_3$, each with a diffraction efficiency greater than 2.5% [8]. The storage of ∿500 holograms with a s/n ratio due to crosstalk of ∿40 dB requires a total angular variation of ∿50 degrees. To attain the same hologram storage density using wavelength selectivity, the equivalent wavelength shift required would be ∿1100 Å. A wavelength range of this magnitude is possible using a dye laser and at least two dyes. It is not a practical solution to the multiple storage of holograms due to the complexity of the dye laser system. In this program we have investigated only the angular selectivity approach to multiple storage.

Three different angular selection devices were used in this program: electric motors, galvanometers [27], and an acousto-optic deflector [28]. The system requirements on these devices are determined primarily by the storage medium thickness and the accessing mode and time required. For high-density, multiple storage, the storage medium will be ∿1 cm thick for which the full width at half maximum of the main Bragg diffraction peak is ∿0.012 degree. The accessing system must servo onto the peak in the diffraction efficiency to compensate for system drift, vibration, etc. Motors and galvanometers are sequential accessing devices which can access individual holograms in times ranging from milliseconds (galvanometers) to seconds (servo motors). In an earlier part of this program the readout of holograms using an acousto-optic deflector was also demonstrated [28]. The current state-of-the-art in deflectors is the paratellurite (TeO_2) deflector which can produce up to 500 fully resolved spots with a 90% diffraction efficiency with an access time of 20 μs.

27. W. Burke and D. L. Staebler, *Volume Holographic Material Device Feasibility for Map Display Applications*, Final Report prepared under Contract No. N62269-72-C-0793 for Naval Air Development Center, June 1973.
28. J. J. Amodei, W. J. Burke, and D. L. Staebler, *Volume Holographic Material Characterization and Device Feasibility for Map Display Applications*, Final Report prepared under Contract No. N62269-71-C-0533, July 1972.

The choice of a particular accessing system will depend upon overall system considerations. For a low-cost, slow ($\sim$1 s) sequential accessing system the servo motor would be preferred. For a high-speed, random access system the acousto-optic deflector is to be preferred. The galvanometer is an intermediate case between these two extremes and should be considered only in those situations where mechanical stability is not a prime consideration.

B. DISPLAY FORMAT

From the point of view of system configuration and ultimate storage capacity, an important consideration is the final form of the display. The two alternatives are (a) direct display, where the light diffracted by the storage medium is used to reconstruct the viewing images without any buffering, and (b) indirect display, where the image is picked up by an electronic device that controls the final display. The major differences are in the diffraction efficiency required from the medium and in the method of color encoding that can be used.

1. Direct Display

There are two approaches to the direct display of images stored as thick phase holograms. They depend on whether a laser or an incoherent source is used to reconstruct the image and project it onto an appropriate viewing screen. In this section, we shall consider the question of whether either of these approaches is a viable alternative for the display of maps.

The advantages of direct display using a laser source are:
- Large angular packing density
- High-resolution readout capability

The disadvantages are:
- Mixed gas or multiple lasers are required for color
- Poor red sensitivity in all known storage media
- Buildup of spurious optical scattering during prolonged readout at high light levels

An incoherent source for the readout of thick phase holograms is an alternative to a laser source since it is simpler and has the advantage of

41

providing the three primary colors from a single source [27]. The measurements and the simple model for incoherent readout discussed in Ref. 27 showed that there were several tradeoffs in the use of an incoherent source. The primary result was that the optimum performance was obtained for a source whose coherence length was of the order of the crystal thickness. For a 0.2-cm-thick crystal this length corresponds to a source bandwidth of 1.5 Å at 5500 Å. Thus, we must seek an incoherent source with brightness comparable to that of a laser over a bandwidth of several angstroms. There are no sources other than the Hg line at 5460 Å which posses a brightness comparable to that found in laser sources.

For a 1000-W Xe arc the energy collected by a lens which subtends a solid angle of 0.32 steradian and which focuses the collected light through a 1/8-in.-diam pinhole (the system used in this work) is approximately 0.16 mW/Å in the visible range. For a 1000-W Hg or Hg-Xe arc the output at 5460 Å is approximately 5 mW/Å. Small Ar$^+$, helium-neon, or helium-cadmium lasers can easily produce outputs larger than these values at the corresponding wavelengths.

In the moving map direct display system developed by RCA Burlington a power density of 132 mW/ft^2 of green light is required on the viewing screen to provide sufficient brightness for viewing in sunlight [29]. For the standard 6-in.-diam viewing screen this corresponds to a total incident power of 25 mW. For the same brightness using blue (4880 Å), and red (6471 Å) laser light from a mixed gas laser would require approximately three times more power at 4880 Å, and approximately five times more power at 6471 Å (estimated from the photo-optic response curve). To obtain a quasi-uniform illumination over the area of the hologram, the Gaussian readout beam is expanded to a 2.54-cm-diam beam. This expanded beam contains 27% of the laser line output power in the 1-cm-diam area of the recorded hologram in the center of the beam. For a typical hologram efficiency of 10% per primary color the overall system efficiency per primary is then 2.7% (assuming all other losses are negligible). This readout system efficiency implies that the required laser output power in the green would be 0.925 W. For the red and blue primary

29. G. T. Burton, B. R. Clay, R. F. Croce, and D. A. Gore, *Laser-Hologram Multicolor Moving Map Display System*, Final Report, Contract N62269-70-C-0080, November 1970.

colors the required laser output powers are $\sim$4.6 and $\sim$2.7 W, respectively.
These output powers are far in excess of those feasible for a cockpit moving
map display primarily because of the electrical power requirements of such
a laser.

For those applications in which electrical power consumption is not a
major constraint, the requirement of separate holograms for each primary
color of an image will provide an upper bound on the effective storage
capacity of a crystal. For a 1-cm-thick crystal the effective storage
capacity would be $\sim$300 holograms in the same volume.

2. Electronic Display

In systems where direct display cannot satisfy overall system require-
ments an electronic display may provide an adequate solution. This approach
includes an electronic pickup, such as a vidicon, and a buffer which decodes
the pickup and provides for proper visual display. Normally, such a system
would include a kinescope for final viewing but is not limited to this
approach.

The advantages of electronic display are several. Among the most im-
portant are:

- Low diffraction efficiency holograms may be used because of
  the high sensitivity of the vidicon pickup. This would result
  in much increased storage capacity.
- Color display can be produced with a variety of formats (one,
  two, or three frames) and require a single wavelength for re-
  cording and readout.
- The sensitivity of the electro-optic medium need be high only
  at one wavelength and not over a broad range of wavelengths.
- Low-power lasers can be used, thus reducing system cost and
  complexity.
- Increased flexibility in the display format and in the addition
  of real-time information to the visual display.

The disadvantages of this approach are:

- The resolution capabilities of the present electronic display
  based on color kinescope are the order of 350 lines with a
  potential increase of up to a factor of two in resolution.

43

● Increased complexity and possible cost in terms of the added
  electronics.

The results obtained with the two-frame color encoding technique [28]
show that this approach should yield, with further effort, a color display
of the required quality. The high optical quality of $LiNbO_3$ crystals appears
to reduce the redundancy required for this application as compared with other
storage materials such as photoresist.

The limited resolution of kinescope displays negates, as noted above, the
high-resolution storage capability of $LiNbO_3$. Systems such as a scanned laser
coupled with a high-resolution vidicon or a light valve are alternative
formats which will have to be considered for higher resolution displays.

Our conclusion based upon the comparison of direct and electronic dis-
plays is that the electronic approach is preferred because of its flexibility,
the high laser power requirements of a direct display, and the fact that the
color encoding technology has already undergone extensive development in the
RCA holotape program.

III. CONCLUSIONS

The research we have conducted over the last 5 years has led to the de-
velopment of Fe-doped $LiNbO_3$ as a versatile volume holographic storage medium
which lends itself well to use in a read-only information retrieval system.
Its principal advantage is that many high resolution fixed holograms can be
stored in a 1-cm-thick crystal. The maximum number is determined by a trade-
off with diffraction efficiency. We have demonstrated the storage of 500
holograms, each with a diffraction efficiency in excess of 2-1/2%. Efficien-
cies of 1% should be readily attainable for 1000 holograms. Storage is done
with an argon ion laser operating at 4880 Å, in a crystal heated to 160°C to
produce fixing simultaneously. The average time required for storage with a
1-W laser is about 15 s per hologram. The fixed holograms have measured life-
times of many years. The signal-to-noise is found to be about 40 dB at the
angular spacings required to achieve high storage capacity. Occasional ex-
posure of the crystal to an incoherent light source is required to erase
spurious optical damage and to maintain this high image quality.

The basic components of an optimal readout system would be based upon the
foregoing discussions of the different components of an information storage
and readout system. They are:

(1) Fe-doped $LiNbO_3$ crystals with stored information.

(2) Low-power Ar^+ ion laser required for readout.

(3) Readout of individual holograms using an acousto-optic
    deflector to perform angular selection.

(4) Readout image detection using a vidicon or Bivicon camera de-
    pending upon whether a monochrome or a color system is required.

(5) Two-frame encoded transparencies or color separations for
    storage of color information.

(6) Kinescope for image display.

The competing systems for a moving map display are (a) direct projection
of maps stored on 35-mm film and (b) direct projection of maps recorded as thin
phase holograms embossed in vinyl which is currently under development by RCA
Burlington. Each of these systems depends upon reel to reel motion of the tape
transport to provide a moving map display. The volume holographic map display

described here provides fast (∿100 μs) random access to the stored maps by use of an acousto-optic deflector and eliminates the possibility of tape breakage. In addition, the fast access allows time sharing of one crystal by a number of viewers. Map motion in this system can be obtained either by motion of the image on the vidicon target with mechanical deflection or by the use of electronic techniques such as a silicon storage tube.

It is clear that the use of volume holographic storage offers a significant advantage in mechanical complexity at the expense of additional electronic complexity. The electronic techniques required are, however, well proven and should not present a significant barrier to the implementation of a volume holographic moving map display system.

REFERENCES

1. D. L. Staebler, W. Phillips, and B. W. Faughnan, *Materials for Phase Holographic Storage*, Final Report, Contract No. N00019-72-C-0147, prepared for Naval Air Systems Command, March 1973.

2. D. L. Staebler and J. J. Amodei, Ferroelectrics **3**, 107 (1972); J. J. Amodei and D. L. Staebler, Appl. Phys. Letters **18**, 540 (1971).

3. B. F. Williams, W. J. Burke, and D. L. Staebler, Appl. Phys. Letters **28**, 224 (1976).

4. W. Burke, W. Phillips, D. L. Staebler, and B. F. Williams, *Materials for Phase Holographic Storage*, Final Report, Contract No. N00019-74-C-0312, prepared for Naval Air Systems Command, April 1975.

5. P. J. Jorgensen and R. W. Bartlett, J. Phys. Chem. Solids **30**, 2639 (1969).

6. J. J. Amodei, W. Phillips, and D. L. Staebler, *Phase Holographic Storage Media for Display Applications*, Final Report, Contract No. N62269-70-C-0372, June 1971.

7. W. Phillips and J. M. Hammer, J. Electronic Materials **4**, 549 (1975).

8. D. L. Staebler, W. J. Burke, W. Phillips, and J. J. Amodei, Appl. Phys. Letters **26**, 182 (1975).

9. W. Phillips, W. J. Burke, and D. L. Staebler, *Materials for Volume Phase Holographic*, Quarterly Report No. 2 prepared for Naval Air Systems Command, under Contract No. N00019-76-C-0116, May 1976.

10. W. J. Burke, W. Phillips, and D. L. Staebler, *Materials for Volume Phase Holography*, Quarterly Report No. 1 prepared for Naval Air Systems Command under Contract No. N00019-76-C-0116, February 1976.

11. W. Phillips, W. J. Burke, and D. L. Staebler, *Materials for Volume Phase Holographic*, Quarterly Report No. 3 prepared Naval Air Systems Command under Contract No. N00019-76-C-0116, August 1976.

12. W. Bollman and N. Gernand, Phys. Stat. Sol. (a) **9**, 301 (1972).

13. J. J. Amodei, RCA Review **32**, 185 (1971).

14. See, e.g., *Handbook on Lasers*, R. J. Pressley, Ed. (Chemical Rubber Co., 1971).

15. H. Kogelnik, Bell Syst. Tech. J. **48**, 2909 (1969).

16. D. L. Staebler and W. Phillips, Appl. Optics **13**, 789 (1974).

17. G. A. Alphonse and W. Phillips, RCA Review **37**, 184 (1976).

18. D. L. Staebler and J. J. Amodei, J. Appl. Phys. **43**, 1042 (1972).

19. R. Parsons, W. D. Cornish, and L. Young, Appl. Phys. Letters **27**, 654 (1975).

20. R. Magnusson and T. K. Gaylord, J. Appl. Phys. **47**, 190 (1976).

21. W. Phillips, J. J. Amodei, and D. L. Staebler, RCA Review **33**, 94 (1972).

REFERENCES (Continued)

22. R. Magnusson and T. K. Gaylord, Appl. Optics 13, 1545 (1974).

23. D. L. Staebler and W. Phillips, Appl. Phys. Letters 24, 263 (1974).

24. W. J. Burke, *S/N Ratio of Holographic Images*, Final Report, Contract No. N00019-75-C-0494, November 1975.

25. W. J. Burke, P. Sheng, and H. A. Weakliem, *Intrinsic Noise Sources in Volume Holography*, Final Report prepared under Contract No. N00014-75-C-0590 for Office of Naval Research, December 1975.

26. A. H. Firester, E. C. Fox, T. Gayeski, W. J. Hannan, and M. Lurie, RCA Review 33, 131 (1972).

27. W. Burke and D. L. Staebler, *Volume Holographic Material Device Feasibility for Map Display Applications*, Final Report prepared under Contract No. N62269-72-C-0793, for Naval Air Development Center, June 1973.

28. J. J. Amodei, W. J. Burke, and D. L. Staebler, *Volume Holographic Materials Characterization and Device Feasibility for Map Display Applications*, Final Report prepared under Contract No. N62269-71-C-0533, July 1972.

29. G. T. Burton, B. R. Clay, R. F. Croce, and D. A. Gore, *Laser-Hologram Multicolor Moving Map Display System*, Final Report, Contract N62269-70-C-0080, November 1970.